Quantitative proteomics reveals oxygen-induced adaptations in Caldalkalibacillus thermarum TA2. A1 microaerobic chemostat cultures

de Jong, S.I.; Wissink, M.; Yildirim, K.; Pabst, Martin; van Loosdrecht, Mark C.M.; McMillan, D.G.G.

DOI
10.3389/fmicb.2024.1468929

Publication date
2024

Document Version
Final published version

Published in
Frontiers in Microbiology

frontiers | Frontiers in Microbiology

TYPE Original Research
PUBLISHED 28 October 2024
DOI 10.3389/fmicb.2024.1468929

OPEN ACCESS

EDITED BY
Noha M. Mesbah,
Suez Canal University, Egypt

REVIEWED BY
Hiroyuki Arai,
The University of Tokyo, Japan
Kazunobu Matsushita,
Yamaguchi University, Japan
Wolfgang Buckel,
University of Marburg, Germany

*CORRESPONDENCE
Samuel I. de Jong
✉ s.i.dejong@tudelft.nl
Duncan G. G. McMillan
✉ d.g.g.mcmillan@tudelft.nl;
d.g.g.mcmillan@reading.ac.uk

RECEIVED 22 July 2024
ACCEPTED 09 September 2024
PUBLISHED 28 October 2024

CITATION
de Jong SI, Wissink M, Yildirim K, Pabst M, van Loosdrecht MCM and McMillan DGG (2024) Quantitative proteomics reveals oxygen-induced adaptations in *Caldalkalibacillus thermarum* TA2.A1 microaerobic chemostat cultures. *Front. Microbiol.* 15:1468929. doi: 10.3389/fmicb.2024.1468929

Quantitative proteomics reveals oxygen-induced adaptations in *Caldalkalibacillus thermarum* TA2.A1 microaerobic chemostat cultures

Samuel I. de Jong[1]*, Martijn Wissink[1], Kadir Yildirim[1], Martin Pabst[1], Mark C. M. van Loosdrecht[1] and Duncan G. G. McMillan[1,2]*

[1]Department of Biotechnology, Delft University of Technology, Delft, Netherlands, [2]School of Biological Sciences, University of Reading, Whiteknights, United Kingdom

The thermoalkaliphile *Caldalkalibacillus thermarum* possesses a highly branched respiratory chain. These primarily facilitate growth at a wide range of dissolved oxygen levels. The aim of this study was to investigate the regulation of *C. thermarum* respiratory chain. *C. thermarum* was cultivated in chemostat bioreactors with a range of oxygen levels (0.25% O_2–4.2% O_2). Proteomic analysis unexpectedly showed that both the type I and the type II NADH dehydrogenase present are constitutive. The two terminal oxidases detected were the cytochrome *c*:oxygen aa_3 oxidase, whose abundance was highest at 4.2% O_2. The cytochrome *c*:oxygen ba_3 oxidase was more abundant at most other O_2 levels, but its abundance started to decline below 0.42% O_2. We expected this would result in the emergence of the cytochrome *c*:oxygen bb_3 complex or the menaquinol:oxygen *bd* complex, the other two terminal oxidases of *C. thermarum*; but neither was detected. Furthermore, the sodium-proton antiporter complex Mrp was downregulated under the lower oxygen levels. Normally, in alkaliphiles, this enzyme is considered crucial for sodium homeostasis. We propose that the existence of a sodium:acetate exporter decreases the requirement for Mrp under strong oxygen limitation.

KEYWORDS

chemostat, regulation, adaptation, alkaliphile, microaerobic, respiration

Introduction

Branched respiratory chains are a common feature in the microbial world. Equipped with alternatives for canonical electron transfer chain (ETC) complexes, microbes can effectively manage fluctuating oxygen conditions encountered within their native environments (Poole and Cook, 2000). As an example, the gut microbe *Escherichia coli* has a terminal bo_3 oxidase for aerobic conditions and two *bd*-type terminal oxidases for anaerobic conditions (Musser et al., 1993; Lindqvist et al., 2000); the latter condition would be encountered more often by *E. coli* (Kaper et al., 2004). While prior research under controlled conditions predominantly focused on model organisms (De Graef et al., 1999; Alexeeva et al., 2002; de Groot et al., 2007; Steinsiek et al., 2011, 2014; Baez et al., 2022), much remains unknown about the regulation of respiratory enzymes of microorganisms from more extreme origins. For instance, the oxic layer of an exotic environment such as a hot spring is confined to the uppermost 1–2 cm (Revsbech and Ward, 1984; Jørgensen and Nelson, 1988) and can undergo diurnal variations

(van der Meer et al., 2005). This environment selects microbes with a branched respiratory chain to adapt to fluctuating oxygen levels. In the case of microbes from hot springs, a compounding challenge is the combined effects of high temperature and extreme pH. The natural habitat of the obligate aerobic thermoalkaliphile *Caldalkalibacillus thermarum* TA2.A1 is an alkaline hot spring with a pH of 10 and 65°C, Mount Te Aroha, New Zealand (Peddie et al., 1999). To cope with the broad spectrum of oxygen concentrations it faces in its native environment, *C. thermarum* has a highly branched proton-mediated ETC (de Jong et al., 2020).

C. thermarum has a putative type I (Ndh-I) and a type II (Ndh-II) NADH dehydrogenase (de Jong et al., 2020). Ndh-I from aerobic bacteria are large proton-pumping multi-subunit integral membrane proteins that regenerate NAD^+ from NADH (Figure 1; Brandt, 2006). In contrast, Ndh-II are small single-subunit peripheral membrane proteins with the same regeneration function but without pumping protons (Figure 1; Melo et al., 2004). The *C. thermarum* Ndh-II is biochemically well-described and is capable of rapid NADH turnover in a membrane environment (Godoy-Hernandez et al., 2019). *C. thermarum* also harbors a succinate dehydrogenase (Sdh) and a putative fumarate reductase (Figure 1; fumarate reductase not depicted; Hederstedt and Rutberg, 1981; Van Hellemond and Tielens, 1994). Little is known about either enzyme in *C. thermarum;* however, Sdh activity has been measured in purified *C. thermarum* membranes (McMillan et al., 2009).

There is a putative hybrid electron-pair splitting Complex III menaquinol:cytochrome *c* oxidoreductase b_6c_1 complex (Cyt. b_6c_1; de Jong et al., 2020). Cyt. b_6c_1 is a hybrid cytochrome with high sequence similarities between the cytochromes bc_1 and b_6f, both of which are integral membrane protein complexes and are found in mitochondrial and cyanobacterial electron transport chains, respectively. Cyt. b_6c_1 serves to transfer electrons from menaquinone to cytochrome *c* (Figure 1; Sone et al., 1996; Saribas et al., 1999). *C. thermarum* also boasts four putative terminal oxidases, all integral membrane proteins (de Jong et al., 2020). Cytochrome aa_3 (Cyt. aa_3), cytochrome ba_3 (Cyt. ba_3), and cytochrome bb_3 (Cyt. bb_3) rely on cytochrome *c* as an electron source (see Figure 1). Cyt. aa_3 is known as an 'aerobic oxidase', typically being expressed under aerobic growth conditions (Von Ballmoos et al., 2012). A model Cyt. aa_3 from *Rhodobacter sphaeroides* pumps protons at an efficiency of 0.7 H^+/electron (Hosler et al., 1992). Cyt. ba_3 and Cyt. bb_3 are not as biochemically well-described as Cyt. aa_3. The *Thermus thermophilus* Cyt. ba_3 and bb_3 both pump protons, but with a lesser efficiency of 0.5 proton per electron transferred to the catalytic site (Pitcher and Watmough, 2004; Von Ballmoos et al., 2012). This leads to speculation that they may differ in oxygen affinity in *C. thermarum*. In support of this, Cyt. bb_3 oxidase allows human pathogens to colonize anoxic tissues and agriculturally important microbes involved in nitrogen fixation (Pitcher and Watmough, 2004). An *Escherichia coli* homolog of the final terminal oxidase, Cytochrome *bd* (Cyt. *bd*), takes its electrons straight from the quinone pool rather than through cytochrome *c* (Figure 1; Asseri et al., 2021), so it is likely the same occurs in *C. thermarum*. In addition, in contrast to the other three oxidases, Cyt. *bd* does not pump any protons.

Finally, completing the ensemble is a proton-coupled F_1F_o-ATP synthase (Cook et al., 2003; McMillan et al., 2007). The *C. thermarum* enzyme is a large multi-subunit integral membrane protein complex that natively unidirectionally synthesizes ATP (McMillan et al., 2007, 2016). The enzyme is highly adapted to function in alkaline pH conditions to be able to recapture protons for ATP synthesis and to be irreversible (Keis et al., 2006; McMillan et al., 2007, 2016; Krah et al., 2023).

Previous investigations into the membrane proteome of *C. thermarum* in the stationary phase of batch cultivation found that Ndh-I, Ndh-II, Sdh, Cyt. b_6c_1, Cyt. aa_3, Cyt. ba_3, and the ATP synthase were expressed (de Jong et al., 2023). However, the regulation of the *C. thermarum* TA2.A1 ETC as a response to differing oxygen availability has never been researched before. To study respiratory regulation as a

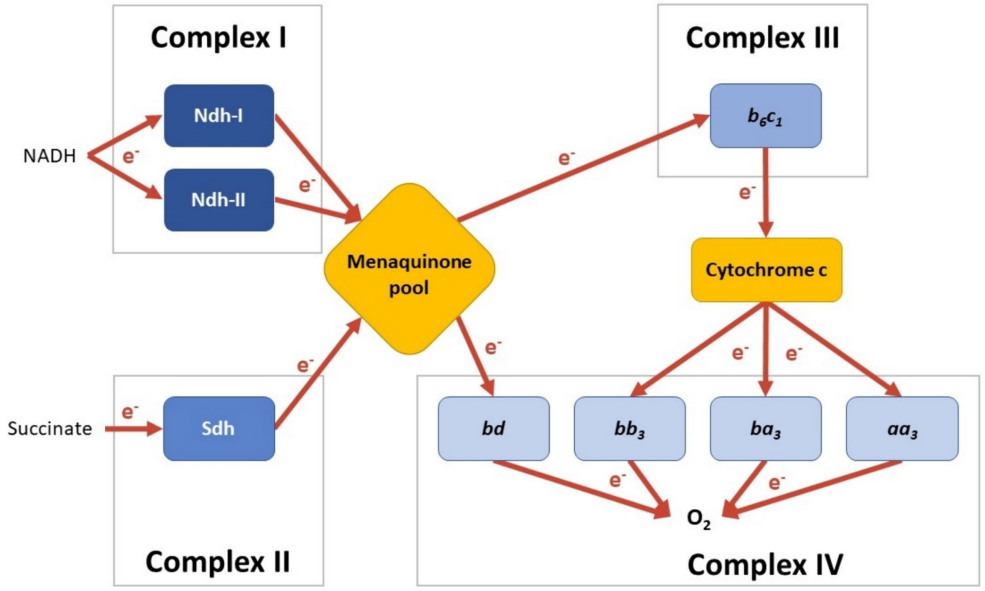

FIGURE 1
Schematic of the menaquinone-mediated *C. thermarum* TA2.A1 electron transport chain (ETC). C. Enzymes are colored per reaction type, and the electron flow is visualized with arrows. Note that currently, no condition is known under which all options are expressed simultaneously.

function of oxygen availability in *C. thermarum* TA2.A1, cultivation in chemostat cultures is required. The use of chemostat bioreactor operation is preferred over other methods as it provides the most replicable results and because it allows precise dosing of oxygen. The term 'aerobiosis' was initially coined for *E. coli* to quantify the microaerobic range using acetate production as a benchmark (Alexeeva et al., 2002). Presumably, in *C. thermarum,* the Ndh-I, Sdh, Cyt. b_6c_1, and Cyt. aa_3 respire the bulk of the electron potential under fully aerobic conditions as this is the most energy-efficient combination available. The primary aim of this study assesses whether that expectation is correct and to test the hypothesis that Ndh-II and the alternative terminal oxidases replace the most energy-efficient respiratory proteins under oxygen limitation. Whole-cell proteomics can then be used to pinpoint the enzymes within the ETC responsible for respiration at every level of aerobiosis.

Distinctive to alkaliphiles is their inverted proton gradient, whereby the internal pH is lower than that of the external environment. This makes proton homeostasis in alkaliphiles a subject that has been studied intensively before (Ito et al., 1997; Aono et al., 1999; Padan et al., 2005; Swartz et al., 2005; Slonczewski et al., 2009). As such, a secondary aim of this study is to determine whether the response to oxygen scarcity is comparable to model organisms. If our hypothesis that *C. thermarum* switches to its alternative ETC proteins proves correct, pH homeostasis must adapt as a result of that. Potential knock-on effects of decreased proton translocation on pH homeostasis in *C. thermarum* TA2.A1 might occur and are an additional area of interest. Finally, this study also aims to pinpoint overarching metabolic changes and benchmark them against model organisms. The multifaceted approach will result in a comprehensive insight into the response of *C. thermarum* to varying oxygen availabilities.

Materials and methods

Cultivation medium

C. thermarum TA2.A1 was cultivated in a medium adapted from an earlier study on the same organism (McMillan et al., 2009). The medium composition in this study was (in g L^{-1}) as follows: tryptone peptone (Difco), 10.0; sucrose, 10; $NaHCO_3$, 9.0; Na_2SO_4, 0.5; K_2HPO_4, 0.2; $(NH_4)_2SO_4$, 0.1; $MgSO_4{\cdot}7\ H_2O$, 0.1; $MnCl_2{\cdot}4\ H_2O$, 5.0×10^{-5}; $ZnSO_4$, 1.4×10^{-5}; $Na_2MoO_4{\cdot}2\ H_2O$, 1.2×10^{-5}. In the case of cultivation in a bioreactor, 0.25 mL L^{-1} of Antifoam C (Sigma-Aldrich, Missouri, United States) was added to the medium. Medium without sucrose was autoclaved at 121°C for 15 min. The pH of the medium was set to 9.5 before autoclaving. Sucrose was autoclaved separately at 110°C in a 50% (w/v) concentrate and added aseptically afterward; basal medium was concentrated during preparation accordingly.

Bioreactor operation

A 3.0 L jacketed bioreactor (Applikon Biotechnology, Netherlands) was used with two Rushton impellers for stirring at 800 rpm, controlled by an ADI 1012 (Applikon Biotechnology, Netherlands). The working volume inside the reactor was kept at 1.0 L by continuous addition of medium and continuous removal of effluent. After an initial batch phase (see below), reactors in this study were operated in a chemostat, with a dilution rate of $D = 0.1\ h^{-1}$. The temperature was kept at 65°C by a thermostat, an Ecoline Staredition E 300 (Lauda, Germany). The reactor was sparged with an air-N_2 mix; to reach the desired aerobiosis level, this mix was altered each time (Table 1). Off-gas was cooled using an RM6S Refrigerated Circulating Bath (Lauda, Germany) as cryostat, and the composition thereof was subsequently measured using an NGA 2000 off-gas multiplexer (Rosemount Inc., Minnesota, USA). The pH was kept stable at 9.5 by the automatic addition of either 2 M H_2SO_4 or 2 M NaOH, controlled by an ADI 1030 Bio Controller (Applikon Biotechnology, Netherlands). Dissolved oxygen was measured with an AppliSens DO probe (Applikon Biotechnology, Netherlands), and the pH was measured using an AppliSens pH+ probe (Applikon Biotechnology, Netherlands), both with a length of 235 mm.

The inoculum for each bioreactor replicate was started by thawing a fresh ±1.6 mL glycerol stock of *C. thermarum* TA2.A1 (frozen at −80°C). All stocks used in this research line originate from the same batch. Thawed cells were reconstituted in a 500 mL round bottom shake flask, with 100 mL working volume, at 65°C and 140 rpm for 18 h. Then, 2% of this culture was transferred to a fresh shake flask containing 100 mL medium and again cultivated for 18 h. The resulting culture was used entirely as reactor inoculum. In the reactor, a batch phase of roughly 8 h followed inoculation, after which the reactor was set to chemostat. Samples were taken periodically for optical density and dry weight measurements; the supernatant was kept at −20°C for acetate and sucrose concentration determination at a later stage. Steady state was assumed when off-gas profiles, OD_{600}, and dry weight measurements were stable for three consecutive retention times. Aseptic conditions were maintained throughout the cultivation procedure. All aeration levels tested were biologically duplicated.

Analytical methods

Optical density measurements were performed at a wavelength of 600 nm (OD_{600}) with a 1 cm light path length in a Biochrom Ultrospec 2,100 Pro UV Vis Spectrometer (Amersham, United Kingdom). For dry weights, a 10 mL sample was filtered over a pre-dried 0.20 µm Supor® PES Membrane Disc Filter (Pall, New York, United States) and dried at 105°C; the filter was weighed before sample addition and after drying for >1 h. Acetate was measured using high-performance liquid chromatography (HPLC). HPLC analysis was performed with 1.5 mmol L^{-1} H_3PO_4 as eluent at a flow of 0.75 mL min^{-1}. The compounds were separated over an Aminex HPX-87H column (BioRad, California, United States) at 59°C and thereafter detected by a refractive ERC RefractoMax 520 (ERC Inc., Japan). Sucrose was

TABLE 1 Required mix of compressed air and nitrogen gas to sparge with desired O_2 concentrations in the bioreactor.

Oxygen level in gas inlet (%)	Air (L_n min^{-1})	Nitrogen gas (L_n min^{-1})
4.2	0.200	0.800
2.05	0.100	0.900
1.05	0.050	0.950
0.42	0.020	0.980
0.25	0.012	0.988

Five conditions were used and can be identified by their final O_2 concentration in the gas inlet. Note these are only the O_2 concentrations in the gas inlet. Regardless of the O_2 concentrations in the inlet gas, the dissolved oxygen concentration was always 0%.

measured using the GOPOD D-Glucose Assay Kit (Megazyme, Ireland), with the addition of 160 mg L^{-1} Grade VII Invertase (300 U mg-1 from *Saccharomyces cerevisiae*; Sigma-Aldrich, Missouri, United States) to the reaction mix. Except for the addition of the invertase enzyme to convert sucrose into glucose, the manufacturer's specifications were followed; the same UV Vis detector was used as for optical density measurements. Analytical measurements were conducted in duplicate.

Protein extraction and proteomics

For proteomics, at the end of each condition, a 100 mg sample (wet weight) was taken and washed in ice-cold phosphate-buffered saline. This sample was flash-frozen in liquid nitrogen and stored thereafter at −80°C until analysis. For analysis, the protocol of which was based on extensive research (den Ridder et al., 2022, 2023), the samples were thawed. Then, 22.2 ± 0.5 mg sample was dissolved in 0.175 mL 1 M triethylammonium bicarbonate buffer in a LoBind tube (Eppendorf, Germany) and thereafter treated exactly according to the 'whole-cell' procedure in our previous study (de Jong et al., 2023). This is also true for shotgun proteomic analysis up to the point where the results were exported as 'proteins.csv' files (Kleikamp et al., 2021; Pabst et al., 2021).

Data processing and visualization techniques

The proteomic data in this study were categorized in two different ways: by Kyoto Encyclopedia of Genes and Genomes (KEGG) modules and the membrane found in our previous study (de Jong et al., 2023), with some proteins falling in both categories. All analyses were performed in Python. Modules were retrieved from the KEGG database using the '*requests*' library; the identifier for *C. thermarum* TA2.A1 genome is '*cthu*'. From the absolute abundances in 'proteins.csv', log2 ratios were calculated to equally assess up- and downregulation under the various conditions; 4.2% O_2 was used as a reference. The resulting data were collected in a single Excel file. This Excel file, containing the proteomics data of each condition and replicate, was subsequently loaded in a *pandas* dataframe and the script was automatically checked which proteins of a certain module were discovered in the shotgun proteomics analysis. In the case of this study, if six or more proteins were found for a specific module in each condition, data were stored in a separate Excel file to make a boxplot. The boxplot was made using the '*matplotlib.pyplot*' library, and settings were adjusted to show the average, whiskers, and outliers. Module names were added manually. For the heat maps of the short-chain fatty acid module (Supplementary Figure S1) or of membrane proteins of interest, the '*visuz*' package of the '*bioinfokit*' library was used. Fake data were added to ensure a $\log_2$ ratio of zero was always the center.

Results and discussion

An overview of the adaptation to oxygen limitation by *C. thermarum* TA2.A1

The goal of this study was to assess the regulation of the *C. thermarum* ETC, uncover potentially alkaliphile-specific adaptation, and assess overarching metabolic changes under varying oxygen availabilities. The first objective was to find the required oxygen level in the gas inlet at which oxygen would become limiting (i.e., dissolved oxygen = 0 at steady state). Preparatory chemostat cultivations were performed at a broader range than reported here; the highest aeration level at which oxygen limitation was detected was 4.2% O_2 in the gas inlet; the lowest oxygen level at which growth was detected was 0.25% O_2 (Supplementary Figures S2, S3). In all of these conditions, the dissolved oxygen concentration was zero, meaning consumed oxygen was limited by the oxygen transfer capacity. For the purpose of this report, *C. thermarum* was grown with five different oxygen levels in the gas mix: 4.2, 2.05, 1.05, 0.42, and 0.25%. As described above, N_2 gas was added to keep gas flow at 1.0 L_n min^{-1}. The biomass-specific substrate consumption rate q_s barely varied at 0.42% O_2 and above: 29.3 $mmol_s$ $Cmol_x^{-1}$ $h^{-1} \leq q_s \leq 38.5$ $mmol_s$ $Cmol_x^{-1}$ h^{-1}. At the 0.25% O_2, an increase was measured: $q_s = 51.0$ $mmol_s$ $Cmol_x^{-1}$ h^{-1}. While all bioreactors operated in oxygen-limited conditions, acetate production only occurred at 2.05% O_2 and lower mole fractions. The biomass-specific acetate production rate q_{ac} varied between 44.2 $mmol_{ac}$ $Cmol_x^{-1}$ h^{-1} and 123.6 $mmol_{ac}$ $Cmol_x^{-1}$ h^{-1}. Although acetate production generally increased with decreasing oxygen, no linear trend was observed, unlike what is described for *E. coli* (Alexeeva et al., 2002). From a basic physiological perspective, *C. thermarum* follows the same strategy to combat oxygen limitation, which is to supplement its failing aerobic respiration with increasing amounts of substrate-level phosphorylation provided by partial acetate fermentation.

Whole-cell proteomics was performed for both replicates of each condition. To determine on a more detailed level whether the regulation under oxygen-limited conditions is comparable to model organisms, proteomics of the highest (4.2% O_2) and lowest (0.25% O_2) levels were compared. Figure 2 shows this regulation per pathway, calculated as $\log_2$ ratios. As stated above, *C. thermarum* uses a different strategy compared to model organisms such as *E. coli* and *S. cerevisiae* to move from respiration to fermentation. The discrepancy between this study and the model organism study stems from the aforementioned stable q_s in this study and the fact that *C. thermarum* cannot grow under absolute anaerobic conditions. Together with the q_s, glycolysis remains stable in *C. thermarum*, while upregulation of glycolysis is generally observed in *E. coli* and *S. cerevisiae* (de Groot et al., 2007; Steinsiek et al., 2011; Ederer et al., 2014) to ensure enough carbon is available to ferment. The partial fermentation of *C. thermarum* to acetate likely stems from the carbon flux being diverted from the TCA cycle to acetate production, without the requirement of significant proteomics reallocations over a whole pathway. Proteomics data show an increase in enzymes responsible for acetate production, Pta and Ack (Supplementary Figure S1), to facilitate the increased carbon flux through that route. Few previous studies tried to also assess anabolic proteomics changes, yet some interesting observations deserve discussion. A few pathways are entirely up- or downregulated more than 2-fold under 0.25% O_2 relative to 4.2% O_2 (i.e., having a $\log_2$ ratio greater than −1 or + 1). Three pathways stand out as being multifold downregulated as a whole: *de novo* pyrimidine biosynthesis and both cobalamin biosynthesis pathways. Enzymes of pyrimidine biosynthesis are known to be 6–20 times more active under anaerobic conditions, as was first reported in *Staphylococcus aureus* (McIllmurray and Lascelles, 1970). A similar increase in enzymatic activity in *C. thermarum* under diminished oxygen conditions should decrease

10.3389/fmicb.2024.1468929

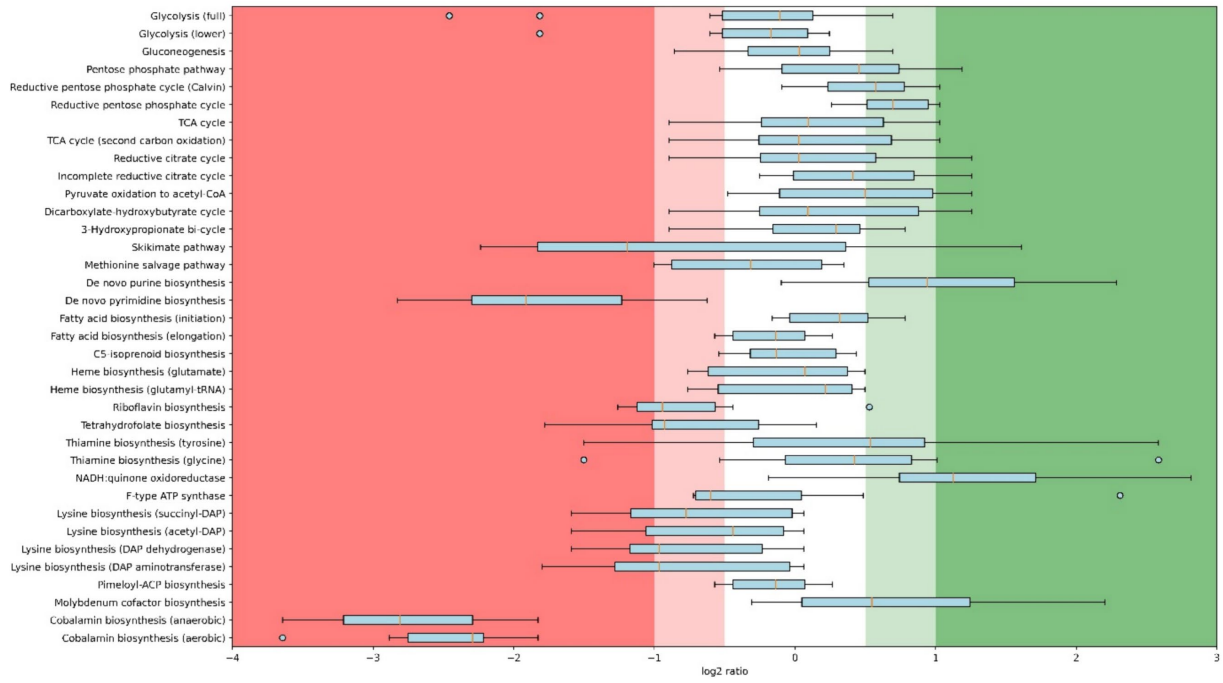

FIGURE 2
Box plot with whisker and outliers comparing proteomics results of 4.2% O_2 (highest level) and 0.25% O_2 (lowest level) chemostats per pathway. Regulation is calculated as $\log_2$ ratios; 0.25% O_2 relative to 4.2% O_2. Displayed pathways are KEGG modules of which at least 2 unique peptides of 6 or more proteins are detected in both conditions. Module names are as descriptive as possible, underlying KEGG identifiers can be found in Supplementary Table S1, and the underlying proteomics data is publicly available (see below).

the production requirement of pyrimidine synthesis proteins, causing the observed downregulation. Cobalamin can be produced both aerobically and anaerobically, and *C. thermarum* contains both pathways. Both of these pathways are downregulated more than 4-fold. Decreased cobalamin production is because cobalamin was involved in protection against reactive oxygen species (ROS) as has been demonstrated in the acidophile *Leptospirillum* Group II *CF*-I (Ferrer et al., 2016). Having this function in *C. thermarum* next to its various regular functions would explain the decreased requirement when oxygen becomes limiting (Neil and Marsh, 1999; Raux et al., 2000). Two modules are completely upregulated more than 2-fold: NADH:menaquinone oxidoreductases, which will be discussed later, and *de novo* purine biosynthesis.

The upregulation of purine biosynthesis in anaerobiosis has been previously shown in *S. cerevisiae* (de Groot et al., 2007). A plausible cause for the upregulation of purine biosynthesis proteins is that its regulatory enzyme, a glutamine 5-phoshophoribosyl-1-pyrophosphate amidotransferase, is oxygen sensitive (Smith et al., 1994). Whether any post-translational modifications exist to prevent intracellular buildup of purines is unknown; however, it is highly likely.

Unraveling the role of the many respiratory enzymes

As mentioned in the previous section, and contrary to expectations, a higher abundance of NADH:menaquinone oxidoreductases was detected at 0.25% O_2 compared to 4.2% O_2. If assessing per subunit though, as detailed in Figure 3, the upregulation is not as stark for Ndh-I. Rather, a few subunits, namely, subunits A, C, and I, have $\log_2$ ratios exceeding 1.5, while the other are closer to 0.5–1.0. It is curious that the subunits are differentially regulated to an extent. Conclusions are somewhat more definitive with Ndh-II, which has a $\log_2$ ratio of 1.8 at 1.05% O_2 (Figure 3). When compared to *E. coli*, in which solely Ndh-II has been shown to be *upregulated* and Ndh-I *downregulated* when oxygen becomes limiting, this result is surprising (Steinsiek et al., 2011). This result puzzles even more considering the type II NADH dehydrogenase of *C. thermarum* has a higher maximum specific activity than its homolog in *E. coli* (Björklöf et al., 2000; Heikal et al., 2014; Blaza et al., 2017; Godoy-Hernandez et al., 2019). Normally, in *E. coli*, the switch to acetate during decreased aerobiosis is coupled to concomitant ethanol fermentation (Alexeeva et al., 2002). This is because while acetate production provides ATP, ethanol is required to regenerate NAD^+. *C. thermarum* is unable to make ethanol. The inability of *C. thermarum* to produce ethanol could explain the higher Ndh-I abundance at lower oxygen levels, though the authors would reason completely switching to Ndh-II would be more efficient. More research is required to fully explain this counterintuitive behavior.

The succinate dehydrogenase (Sdh) and the F_1F_o-ATP synthase were downregulated, following the same protein presence patterns detailed for *E. coli* (Figure 3; Ederer et al., 2014). Downregulation of Sdh is another contributing factor to the observed acetate production. The inability to fully utilize the TCA cycle dictates that pyruvate should be consumed by another pathway. *E. coli* does not have any genes encoding for a Complex III, but *S. cerevisiae* does. In a previous yeast study (de Groot et al., 2007), its cytochrome bc_1 complex is reported to be downregulated but sadly not to what extent. In this study, *C. thermarum*'s Complex III, the

10.3389/fmicb.2024.1468929

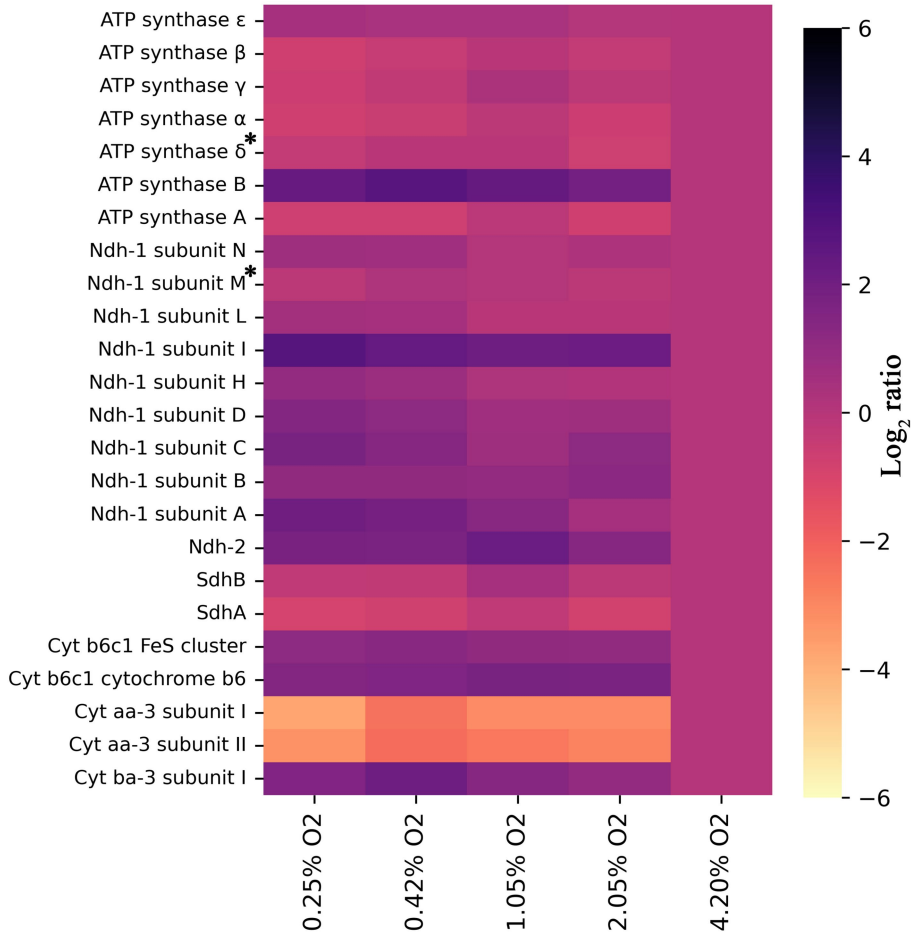

FIGURE 3
Heat map showing $\log_2$ ratios of all detected subunits of the ETC for each condition, provided two or more unique peptides were detected, relative to 4.2% O_2. All trends have a significance of $p < 0.05$, except those denoted with an asterisk. For ATP synthase subunit *δ*, the $p = 0.058$, and for Ndh-1 subunit M, the $p = 0.150$. For all others, the exact significances and the corresponding protein number can be found in Supplementary material S1 and the locus tags in Supplementary Table S1.

cytochrome b_6c_1 complex, is slightly upregulated at lower O_2 levels. This observation could be related to the aforementioned upregulation of Ndh-I. Another potential explanation for Ndh-I upregulation and F_1F_o-ATP synthase repression at low O_2 is that the intracellular pH may be increased to keep the redox homeostasis. Babauta et al. (2012) suggested intracellular pH could modify redox potential by virtue of low oxygen concentration decreasing intracellular ROS concentration (Baez and Shiloach, 2013) and increasing NADPH content (Baez and Shiloach, 2017) and, in this theory, would be very subtle, because pH in itself is also a strong regulatory mechanism in the context of alkaliphile. In this context, it is unsurprising that the epsilon subunit of the *C. thermarum* F_1F_o-ATP synthase, an enzyme with the capability of proton pumping, is heavily regulated by pH (Krah et al., 2023).

Two types of terminal oxidases were detected in this experiment, in fact in all conditions: Cyt. aa_3 and Cyt. ba_3. As expected, Cyt. aa_3 is downregulated when oxygen becomes limiting, while Cyt. ba_3 is upregulated (Figure 3). The main difference between these two enzymes is that Cyt. aa_3 allows for the translocation of 2 H^+ per 2 e^-, while Cyt. ba_3 only translocates 1 H^+ per 2 e^-. As described in the introduction, a similar pattern is observed in *E. coli*. This organism switches from its cytochrome bo_3 (pumping 1H^+/electron), through cytochrome *bd* (pumping 0H^+/electron) and finally to cytochrome *bd*-II (pumping 0H^+/electron) under increasing anaerobiosis (Steinsiek et al., 2011, 2014). Although the abundance of Cyt. ba_3 in this study starts to tail of below 0.42% O_2, no other terminal oxidase was detected. This is likely due to the hydrophobicity of both proteins and accessibility to proteolytic digestion, a major challenge in membrane proteomics. Regardless, based on our findings of aa_3 and ba_3, it seems most likely that Cyt. bb_3 or Cyt. *bd* takes over responsibility for oxygen electron transfer at oxygen concentrations less than 0.25%. Cyt. bb_3, as described in the introduction, allows human pathogens to colonize anoxic tissues and translocates 1 H^+ per electron pair, but possibly with a higher affinity since it is expressed at lower O_2 concentrations. Cyt. *bd* is also known to be used at low oxygen conditions in *E. coli* (Steinsiek et al., 2011; Ederer et al., 2014).

Is a low oxygen adaptation specific for alkaliphiles?

In addition to the respiratory chain which is obligately coupled to oxygen, other membrane processes also adapt at different oxygen availabilities (Figure 4). Figure 4 shows the $\log_2$ ratios for transporters

detected in this study and our previous study on unraveling the membrane proteome of this organism (de Jong et al., 2023). There is a striking 6-fold upregulation of CopA, the ATP-coupled copper export mechanism linearly coupled to oxygen limitation (Figure 4). Copper can be toxic to cells, and in *Rubrivivax gelatinosus*, it has been demonstrated that CopA mutants have decreased cytochrome *c* oxidase activity (Azzouzi et al., 2013). The solubility of copper is lower at high pH than under the conditions used in *R. gelatinosus* (Cuppett et al., 2006), perhaps further exacerbating this issue. In addition to this, copper efflux might be induced in *C. thermarum* to protect iron–sulfur cluster enzymes from copper mis-metallation (Fung et al., 2013; Imlay, 2014). This is because the intracellular labile Fe^{2+} pool is higher under oxygen limitation, which leads to a net increase of Fe^{2+}-Fur activity with concomitant iron-protein expression (Beauchene et al., 2017). This gains feasibility, especially considering the ionic radii of Fe^{2+} is 0.076 nm vs. Cu^{2+} 0.073 nm and Cu^{1+} at 0.077 nm (Cotton et al., 1999). Finally, another possible scenario is that the copper requirement of the cell decreases at lower oxygen levels, due to the decreased Cyt aa_3 production, for which copper is required. While Cyt. ba_3, also requiring copper, is produced as an alternative, the absolute amount of each individual enzyme can differ quite starkly; data in this study only show the regulation of proteins relative to themselves. A decreased content of heme-copper oxidases could increase the need for copper export and thus explain the observed pattern. In contrast, the manganese transport complex Mnt is downregulated 6-fold. Generally, manganese is required for living with oxygen (Horsburgh et al., 2002), explaining the lower requirement at low O_2.

Aside from Mnt, the transporter Mrp is also significantly downregulated at lower O_2 concentrations. The Mrp antiporter facilitates the export of Na^+ coupled with the import of H^+. This antiporter is considered a vital protein for alkaliphiles as it is one of the primary methods to regulate internal sodium *and* proton levels (Padan et al., 2001, 2005; Swartz et al., 2005). Data on the ETC show that proton export does not decrease to the extent that Mrp becomes useless. Another reason must drive the decreased need for sodium:proton antiport through Mrp. Since all other medium components remained the same, we especially expect sodium stress to remain as compelling for an alkaliphile such as *C. thermarum* TA2.A1 under low O_2. Interestingly enough, the very first studies into *C. thermarum* TA2.A1 centered on the fact that substrate import (glutamate and sucrose) is mediated using sodium ions, not protons (Peddie et al., 1999, 2000). Though no *in vivo* nor *in vitro* data are reported regarding acetate export, the expectation is that this is also mediated by sodium ions (de Jong et al., 2020). Considering the high level of acetate production at low O_2 levels, we hypothesize that the function of Mrp is—at least partly—replaced by the acetate exporter under these conditions. This would constitute a valuable addition to the field of alkaliphiles as no such regulation of Mrp, to the best of our knowledge, has been found previously.

Conclusion

C. thermarum TA2.A1 was successfully cultivated within a microaerobic range in chemostats, demonstrating its low oxygen requirement. Oxygen limitation became evident near 4.2% O_2 in the gas inlet, while the microorganism grew even at 0.25% O_2 in the gas inlet. Acetate is produced concurrently with respiration to complement

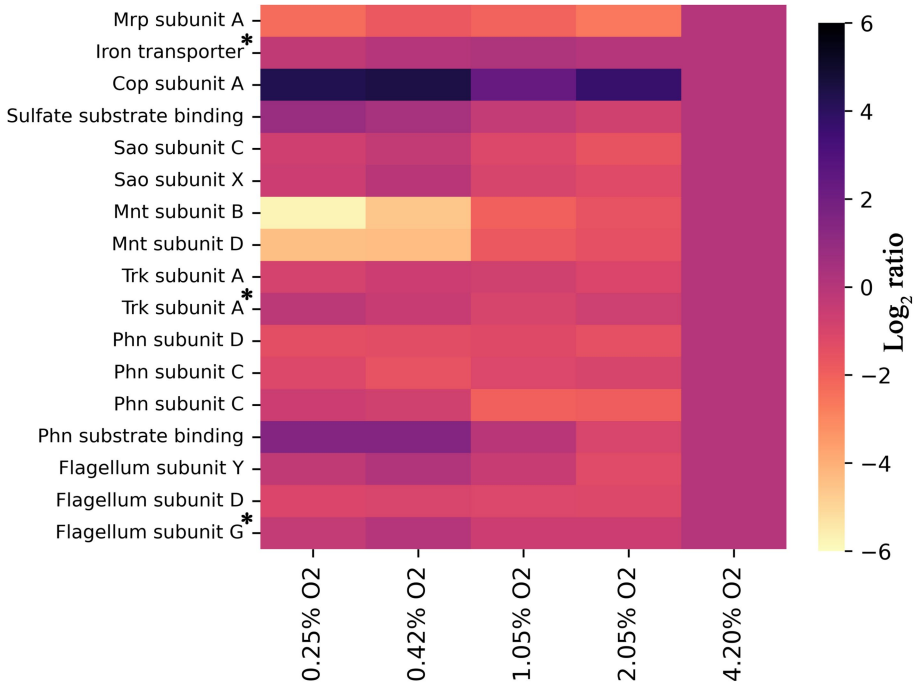

FIGURE 4
Heat map showing $\log_2$ ratios of all detected subunits of known transporters of inorganic compounds for each condition, provided two or more unique peptides were detected, relative to 4.2% O_2. All trends have a significance of $p < 0.05$, except those denoted with an asterisk. For the iron transporter $p = 0.255$, for the Trk subunit A $p = 0.053$, and for the Flagellum subunit G $p = 0.101$. For all others, the exact significances and the corresponding protein number can be found in Supplementary material S1 and the locus tags in Supplementary Table S1.

energy generation. Surprisingly, proteomics data showed that both NADH dehydrogenases are constitutively expressed under the conditions tested. It makes little sense that an Ndh-I is upregulated at low O_2, pumping out protons, when the F_1F_o-ATP synthase that takes the protons back into the cell is downregulated under the same conditions. One potential explanation is that the intracellular pH should be increased at low O_2 to keep the redox homeostasis functional.

Cyt. aa_3 is the predominant contributor to the terminal oxidase pool at the highest oxygen level, while Cyt. ba_3 takes over below 4.2% O_2. Detection of either Cyt. bb_3 or Cyt. *bd* was expected at 0.25% O_2, given that the abundance of Cyt. ba_3 started to decline. Neither Cyt. bb_3 nor Cyt. *bd* was detected, but there is a probability that either or both are present at low oxygen levels. Proteomics analysis of membrane proteins needs to be further developed to fully use this methodology for the study of respiratory systems. Finally, a notable finding was a decreased abundance of the Mrp complex, considered a crucial cog in alkaliphilic sodium homeostasis. We hypothesized that this could be due to the presence of an acetate:sodium symporter, responsible for facilitating acetate export and thereby decreasing sodium stress.

Data availability statement

The datasets presented in this study can be found in online repositories. The names of the repository/repositories and accession number(s) can be found in the article/Supplementary material.

Author contributions

SJ: Data curation, Formal analysis, Investigation, Writing – original draft, Writing – review & editing. MW: Investigation, Writing – original draft. KY: Investigation, Writing – original draft. MP: Data curation, Formal analysis, Software, Validation, Writing – original draft. ML: Funding acquisition, Resources, Supervision, Writing – original draft, Writing – review & editing. DM: Conceptualization, Funding acquisition, Methodology, Project administration, Resources, Supervision, Validation, Writing – original draft, Writing – review & editing.

Funding

The author(s) declare that financial support was received for the research, authorship, and/or publication of this article. The study of SJ was funded by the SIAM Gravitation Grant from the Netherlands Organization for Scientific Research (024.002.002).

Acknowledgments

The authors would like to thank Dimitry Sorokin for valuable discussions and Dita Heikens for helping with proteomics.

Conflict of interest

The authors declare that the research was conducted in the absence of any commercial or financial relationships that could be construed as a potential conflict of interest.

The author(s) declared that they were an editorial board member of Frontiers, at the time of submission. This had no impact on the peer review process and the final decision.

Publisher's note

All claims expressed in this article are solely those of the authors and do not necessarily represent those of their affiliated organizations, or those of the publisher, the editors and the reviewers. Any product that may be evaluated in this article, or claim that may be made by its manufacturer, is not guaranteed or endorsed by the publisher.

Supplementary material

The Supplementary material for this article can be found online at: https://www.frontiersin.org/articles/10.3389/fmicb.2024.1468929/full#supplementary-material

References

Alexeeva, S., Hellingwerf, K. J., and Teixeira de Mattos, M. J. (2002). Quantitative assessment of oxygen availability: perceived aerobiosis and its effect on flux distribution in the respiratory chain of *Escherichia coli*. *J. Bacteriol.* 184, 1402–1406. doi: 10.1128/JB.184.5.1402-1406.2002

Aono, R., Ito, M., and Machida, T. (1999). Contribution of the cell wall component teichuronopeptide to pH homeostasis and alkaliphily in the alkaliphile *Bacillus lentus* C-125. *J. Bacteriol.* 181, 6600–6606. doi: 10.1128/jb.181.21.6600-6606.1999

Asseri, A. H., Godoy-Hernandez, A., Goojani, H. G., Lill, H., Sakamoto, J., McMillan, D. G. G., et al. (2021). Cardiolipin enhances the enzymatic activity of cytochrome bd and cytochrome Bo 3 solubilized in dodecyl-maltoside. *Sci. Rep.* 11, 1–8. doi: 10.1038/s41598-021-87354-0

Azzouzi, A., Steunou, A. S., Durand, A., Khalfaoui-Hassani, B., Bourbon, M., Astier, C., et al. (2013). Coproporphyrin III excretion identifies the anaerobic coproporphyrinogen III oxidase HemN as a copper target in the cu+-ATPase mutant copA- of *Rubrivivax gelatinosus*. *Mol. Microbiol.* 88, 339–351. doi: 10.1111/mmi.12188

Babauta, J. T., Nguyen, H. D., Harrington, T. D., Renslow, R., and Beyenal, H. (2012). pH, redox potential and local biofilm potential microenvironments within *Geobacter sulfurreducens* biofilms and their roles in electron transfer. *Biotechnol. Bioeng.* 109, 2651–2662. doi: 10.1002/bit.24538

Baez, A., Sharma, A. K., Bryukhanov, A., Anderson, E. D., Rudack, L., Olivares-Hernández, R., et al. (2022). Iron availability enhances the cellular energetics of aerobic *Escherichia coli* cultures while upregulating anaerobic respiratory chains. *New Biotechnol.* 71, 11–20. doi: 10.1016/j.nbt.2022.06.004

Baez, A., and Shiloach, J. (2013). *Escherichia coli* avoids high dissolved oxygen stress by activation of SoxRS and manganese-superoxide dismutase. *Microb. Cell Factories* 12, 1–9. doi: 10.1186/1475-2859-12-23

Baez, A., and Shiloach, J. (2017). Increasing dissolved-oxygen disrupts iron homeostasis in production cultures of *Escherichia coli*. *Antonie van Leeuwenhoek* 110, 115–124. doi: 10.1007/s10482-016-0781-7

Beauchene, N. A., Mettert, E. L., Moore, L. J., Keleş, S., Willey, E. R., and Kiley, P. J. (2017). O2 availability impacts iron homeostasis in *Escherichia coli*. *Proc. Natl. Acad. Sci. USA* 114, 12261–12266. doi: 10.1073/pnas.1707189114

Björklöf, K., Zickermann, V., and Finel, M. (2000). Purification of the 45 kDa, membrane bound NADH dehydrogenase of *Escherichia coli* (NDH-2) and analysis of its interaction with ubiquinone analogues. *FEBS Lett.* 467, 105–110. doi: 10.1016/S0014-5793(00)01130-3

Blaza, J. N., Bridges, H. R., Aragão, D., Dunn, E. A., Heikal, A., Cook, G. M., et al. (2017). The mechanism of catalysis by type-II NADH:quinone oxidoreductases. *Sci. Rep.* 7, 1–11. doi: 10.1038/srep40165

Brandt, U. (2006). Energy converting NADH:quinone oxidoreductase (complex I). *Annu. Rev. Biochem.* 75, 69–92. doi: 10.1146/annurev.biochem.75.103004.142539

Cook, G. M., Keis, S., Morgan, H. W., Von Ballmoos, C., Matthey, U., Kaim, G., et al. (2003). Purification and biochemical characterization of the F_1F_O-ATP synthase from Thermoalkaliphilic *Bacillus* sp. strain TA2.A1. *Society* 185, 4442–4449. doi: 10.1128/JB.185.15.4442-4449.2003

Cotton, F. A., Wilkinson, G., Murillo, C. A., and Bochmann, M. (1999). Advanced inorganic chemistry. United States of America: John Wiley & Sons.

Cuppett, J. D., Duncan, S. E., and Dietrich, A. M. (2006). Evaluation of copper speciation and water quality factors that affect aqueous copper tasting response. *Chem. Senses* 31, 689–697. doi: 10.1093/chemse/bjl010

De Graef, M. R., Alexeeva, S., Snoep, J. L., and Teixeira De Mattos, M. J. (1999). The steady-state internal redox state (NADH/NAD) reflects the external redox state and is correlated with catabolic adaptation in *Escherichia coli*. *J. Bacteriol.* 181, 2351–2357. doi: 10.1128/jb.181.8.2351-2357.1999

de Groot, M. J. L., Daran-Lapujade, P., van Breukelen, B., Knijnenburg, T. A., de Hulster, E. A. F., Reinders, M. J. T., et al. (2007). Quantitative proteomics and transcriptomics of anaerobic and aerobic yeast cultures reveals post-transcriptional regulation of key cellular processes. *Microbiology* 153, 3864–3878. doi: 10.1099/mic.0.2007/009969-0

de Jong, S. I., Sorokin, D. Y., van Loosdrecht, M. C. M., Pabst, M., and Mcmillan, D. G. G. (2023). Membrane proteome of the thermoalkaliphile *Caldalkalibacillus thermarum* TA2.A1. *Front. Microbiol.* 14:1228266. doi: 10.3389/fmicb.2023.1228266

de Jong, S. I., van den Broek, M. A., Merkel, A. Y., de la Torre Cortes, P., Kalamorz, F., Cook, G. M., et al. (2020). Genomic analysis of *Caldalkalibacillus thermarum* TA2.A1 reveals aerobic alkaliphilic metabolism and evolutionary hallmarks linking alkaliphilic bacteria and plant life. *Extremophiles* 24, 923–935. doi: 10.1007/s00792-020-01205-w

den Ridder, M., Knibbe, E., van den Brandeler, W., Daran-Lapujade, P., and Pabst, M. (2022). A systematic evaluation of yeast sample preparation protocols for spectral identifications, proteome coverage and post-isolation modifications. *J. Proteome* 261:104576. doi: 10.1016/j.jprot.2022.104576

den Ridder, M., van den Brandeler, W., Altiner, M., Daran-Lapujade, P., and Pabst, M. (2023). Proteome dynamics during transition from exponential to stationary phase under aerobic and anaerobic conditions in yeast. *Mol. Cell. Proteomics* 22:100552. doi: 10.1016/j.mcpro.2023.100552

Ederer, M., Steinsiek, S., Stagge, S., Rolfe, M. D., Ter Beek, A., Knies, D., et al. (2014). A mathematical model of metabolism and regulation provides a systems-level view of how *Escherichia coli* responds to oxygen. *Front. Microbiol.* 5, 1–12. doi: 10.3389/fmicb.2014.00124

Ferrer, A., Rivera, J., Zapata, C., Norambuena, J., Sandoval, Á., Chávez, R., et al. (2016). Cobalamin protection against oxidative stress in the acidophilic iron-oxidizing bacterium Leptospirillum group II CF-1. *Front. Microbiol.* 7, 1–11. doi: 10.3389/fmicb.2016.00748

Fung, D. K. C., Lau, W. Y., Chan, W. T., and Yan, A. (2013). Copper efflux is induced during anaerobic amino acid limitation in *escherichia coli* to protect iron-sulfur cluster enzymes and biogenesis. *J. Bacteriol.* 195, 4556–4568. doi: 10.1128/JB.00543-13

Godoy-Hernandez, A., Tate, D. J., and McMillan, D. G. G. (2019). Revealing the membrane-bound catalytic oxidation of NADH by the drug target type-II NADH dehydrogenase. *Biochemistry* 58, 4272–4275. doi: 10.1021/acs.biochem.9b00752

Hederstedt, L., and Rutberg, L. (1981). Succinate dehydrogenase-a comparative review. *Microbiol. Rev.* 45, 542–555. doi: 10.1128/mr.45.4.542-555.1981

Heikal, A., Nakatani, Y., Dunn, E., Weimar, M. R., Day, C. L., Baker, E. N., et al. (2014). Structure of the bacterial type II NADH dehydrogenase: a monotopic membrane protein with an essential role in energy generation. *Mol. Microbiol.* 91, 950–964. doi: 10.1111/mmi.12507

Horsburgh, M. J., Wharton, S. J., Karavolos, M., and Foster, S. J. (2002). Manganese: elemental defence for a life with oxygen? *Trends Microbiol.* 10, 496–501. doi: 10.1016/S0966-842X(02)02462-9

Hosler, J. P., Fetter, J., Tecklenburg, M. M. J., Espe, M., Lerma, C., and Ferguson-Miller, S. (1992). Cytochrome aa3 of *Rhodobacter sphaeroides* as a model for mitochondrial cytochrome c oxidase. Purification, kinetics, proton pumping, and spectral analysis. *J. Biol. Chem.* 267, 24264–24272. doi: 10.1016/s0021-9258(18)35760-0

Imlay, J. A. (2014). The mismetallation of enzymes during oxidative stress. *J. Biol. Chem.* 289, 28121–28128. doi: 10.1074/jbc.R114.588814

Ito, M., Guffanti, A. A., Zemsky, J., Ivey, D. M., and Krulwich, T. A. (1997). Role of the nhaC-encoded Na+/H+ antiporter of alkaliphilic *Bacillus firmus* OF4. *J. Bacteriol.* 179, 3851–3857. doi: 10.1128/jb.179.12.3851-3857.1997

Jørgensen, B. B., and Nelson, D. C. (1988). Bacterial zonation, photosynthesis, and spectral light distribution in hot spring microbial mats of Iceland. *Microb. Ecol.* 16, 133–147. doi: 10.1007/BF02018909

Kaper, J. B., Nataro, J. P., and Mobley, H. L. T. (2004). Pathogenic *Escherichia coli*. *Nat. Rev. Microbiol.* 2, 123–140. doi: 10.1038/nrmicro818

Keis, S., Stocker, A., Dimroth, P., and Cook, G. M. (2006). Inhibition of ATP hydrolysis by thermoalkaliphilic F_1F_O-ATP synthase is controlled by the C terminus of the ε subunit. *J. Bacteriol.* 188, 3796–3804. doi: 10.1128/JB.00040-06

Kleikamp, H. B. C., Pronk, M., Tugui, C., Guedes da Silva, L., Abbas, B., Lin, Y. M., et al. (2021). Database-independent de novo metaproteomics of complex microbial communities. *Cell Syst.* 12, 375–383.e5. doi: 10.1016/j.cels.2021.04.003

Krah, A., Vogelaar, T., de Jong, S. I., Claridge, J. K., Bond, P. J., and McMillan, D. G. G. (2023). ATP binding by an F1Fo ATP synthase ε subunit is pH dependent, suggesting a diversity of ε subunit functional regulation in bacteria. *Front. Mol. Biosci.* 10, 1–11. doi: 10.3389/fmolb.2023.1059673

Lindqvist, A., Membrillo-Hernández, J., Poole, R. K., and Cook, G. M. (2000). Roles of respiratory oxidases in protecting *Escherichia coli* K12 from oxidative stress. *Antonie van Leeuwenhoek* 78, 23–31. doi: 10.1023/A:1002779201379

McIllmurray, M. B., and Lascelles, J. (1970). Anaerobiosis and the activity of enzymes of pyrimidine biosynthesis in *Staphylococcus aureus*. *J. Gen. Microbiol.* 64, 269–277. doi: 10.1099/00221287-64-3-269

McMillan, D. G. G., Keis, S., Berney, M., and Cook, G. M. (2009). Nonfermentative Thermoalkaliphilic growth is restricted to alkaline environments. *Appl. Environ. Microbiol.* 75, 7649–7654. doi: 10.1128/AEM.01639-09

McMillan, D. G. G., Keis, S., Dimroth, P., and Cook, G. M. (2007). A specific adaptation in the a subunit of thermoalkaliphilic F_1F_O-ATP synthase enables ATP synthesis at high pH but not at neutral pH values. *J. Biol. Chem.* 282, 17395–17404. doi: 10.1074/jbc.M611709200

McMillan, D. G. G., Watanabe, R., Ueno, H., Cook, G. M., and Noji, H. (2016). Biophysical characterization of a thermoalkaliphilic molecular motor with a high stepping torque gives insight into evolutionary atp synthase adaptation. *J. Biol. Chem.* 291, 23965–23977. doi: 10.1074/jbc.M116.743633

Melo, A. M. P., Bandeiras, T. M., and Teixeira, M. (2004). New insights into type II NAD(P)H:Quinone oxidoreductases new insights into type II NAD(P)H:Quinone oxidoreductases. *Microbiol. Mol. Biol. Rev.* 68, 603–616. doi: 10.1128/MMBR.68.4.603

Musser, S. M., Stowell, M. H. B., and Chan, S. I. (1993). Further comparison of ubiquinol and cytochrome c terminal oxidases. *FEBS Lett.* 335, 296–298. doi: 10.1016/0014-5793(93)80751-F

Neil, E., and Marsh, G. (1999). Coenzyme B_{12} (cobalamin)-dependent enzymes. *Essays Biochem.* 34, 139–154. doi: 10.1042/bse0340139

Pabst, M., Grouzdev, D. S., Lawson, C. E., Kleikamp, H. B. C., de Ram, C., Louwen, R., et al. (2021). A general approach to explore prokaryotic protein glycosylation reveals the unique surface layer modulation of an anammox bacterium. *ISME J.* 16, 346–357. doi: 10.1038/s41396-021-01073-y

Padan, E., Bibi, E., Ito, M., and Krulwich, T. A. (2005). Alkaline pH homeostasis in bacteria: new insights. *Biochim. Biophys. Acta Biomembr.* 1717, 67–88. doi: 10.1016/j.bbamem.2005.09.010

Padan, E., Venturi, M., Gerchman, Y., and Dover, N. (2001). Na^+/H^+ antiporters. *Biochim. Biophys. Acta Bioenerg.* 1505, 144–157. doi: 10.1016/S0005-2728(00)00284-X

Peddie, C. J., Cook, G. M., and Morgan, H. W. (1999). Sodium-dependent glutamate uptake by an Alkaliphilic, thermophilic *Bacillus* strain, TA2.A1. *J. Bacteriol.* 181, 3172–3177. doi: 10.1128/JB.181.10.3172-3177.1999

Peddie, C. J., Cook, G. M., and Morgan, H. W. (2000). Sucrose transport by the alkaliphilic, thermophilic *Bacillus* sp. strain TA2.A1 is dependent on a sodium gradient. *Extremophiles* 4, 291–296. doi: 10.1007/s007920070016

Pitcher, R. S., and Watmough, N. J. (2004). The bacterial cytochrome cbb3 oxidases. *Biochim. Biophys. Acta Bioenerg.* 1655, 388–399. doi: 10.1016/j.bbabio.2003.09.017

Poole, R. K., and Cook, G. M. (2000). Redundancy of aerobic respiratory chains in bacteria? Routes, reasons and regulation. *Adv. Microb. Physiol.* 43, 165–224. doi: 10.1016/s0065-2911(00)43005-5

Raux, E., Schubert, H. L., and Warren, M. J. (2000). Biosynthesis of cobalamin (vitamin B_{12}): a bacterial conundrum. *Cell. Mol. Life Sci.* 57, 1880–1893. doi: 10.1007/PL00000670

Revsbech, N. P., and Ward, D. M. (1984). Microelectrode studies of interstitial water chemistry and photosynthetic activity in a hot spring microbial mat. *Appl. Environ. Microbiol.* 48, 270–275. doi: 10.1128/aem.48.2.270-275.1984

Saribas, A. S., Mandaci, S., and Daldal, F. (1999). An engineered cytochrome b_6c_1 complex with a split cytochrome *b* is able to support photosynthetic growth of *Rhodobacter capsulatus*. *J. Bacteriol.* 181, 5365–5372. doi: 10.1128/jb.181.17.5365-5372.1999

Slonczewski, J. L., Fujisawa, M., Dopson, M., and Krulwich, T. A. (2009). Cytoplasmic pH measurement and homeostasis in Bacteria and Archaea. *Adv. Microb. Physiol.* 55, 1–317. doi: 10.1016/S0065-2911(09)05501-5

Smith, J. L., Zaluzec, E. J., Wery, J. P., Niu, L., Switzer, R. L., Zalkin, H., et al. (1994). Structure of the allosteric regulatory enzyme of purine biosynthesis. *Science* 264, 1427–1433. doi: 10.1126/science.8197456

Sone, N., Tsuchiya, N., Inoue, M., and Noguchi, S. (1996). *Bacillus stearothermophilus qcr* operon encoding Rieske FeS protein, cytochrome b_6, and a novel-type cytochrome c_1 of Quinolcytochrome *c* reductase. *J. Biol. Chem.* 271, 12457–12462. doi: 10.1074/jbc.271.21.12457

Steinsiek, S., Frixel, S., Stagge, S., and Bettenbrock, K. (2011). Characterization of *E. coli* MG1655 and frdA and sdhC mutants at various aerobiosis levels. *J. Biotechnol.* 154, 35–45. doi: 10.1016/j.jbiotec.2011.03.015

Steinsiek, S., Stagge, S., and Bettenbrock, K. (2014). Analysis of *Escherichia coli* mutants with a linear respiratory chain. *PLoS One* 9, 1–15. doi: 10.1371/journal.pone.0087307

Swartz, T. H., Ikewada, S., Ishikawa, O., Ito, M., and Krulwich, T. A. (2005). The Mrp system: a giant among monovalent cation/proton antiporters? *Extremophiles* 9, 345–354. doi: 10.1007/s00792-005-0451-6

van der Meer, M. T. J., Schouten, S., Bateson, M. M., Nübel, U., Wieland, A., Kühl, M., et al. (2005). Diel variations in carbon metabolism by green nonsulfur-like bacteria in alkaline siliceous hot spring microbial mats from Yellowstone National Park. *Appl. Environ. Microbiol.* 71, 3978–3986. doi: 10.1128/AEM.71.7.3978-3986.2005

Van Hellemond, J. J., and Tielens, A. G. M. (1994). Expression and functional properties of fumarate reductase. *Biochem. J.* 304, 321–331. doi: 10.1042/bj3040321

Von Ballmoos, C., Ädelroth, P., Gennis, R. B., and Brzezinski, P. (2012). Proton transfer in Ba 3 cytochrome c oxidase from *Thermus thermophilus*. *Biochim. Biophys. Acta Bioenerg.* 1817, 650–657. doi: 10.1016/j.bbabio.2011.11.015